Botanical Journal of the Linnean Society, 2019, **191**, 421–439. With 10 figures.

Carpellary appendages in *Nymphaea* and *Victoria* (Nymphaeaceae): evidence of their role as osmophores based on morphology, anatomy and ultrastructure

LUCÍA MELISA ZINI[1,2,*], BEATRIZ GLORIA GALATI[3], MARINA GOTELLI[3], GABRIELA ZARLAVSKY[3] and MARÍA SILVIA FERRUCCI[1,2]

[1]*Instituto de Botánica del Nordeste (UNNE-CONICET), Corrientes, Argentina*
[2]*Consejo Nacional de Investigaciones Científicas y Técnicas (CONICET), Buenos Aires, Argentina*
[3]*Cátedra de Botánica General, Depto. de Recursos Naturales y Ambiente, Facultad de Agronomía, Universidad de Buenos Aires, Buenos Aires, Argentina*

Received 27 May 2019; revised 19 August 2019; accepted for publication 21 September 2019

In flowers of *Nymphaea* and *Victoria*, carpellary appendages are regarded as structures related to pollination by deceit of night-blooming species. In this study, the anatomy, histochemistry and ultrastructure of carpellary appendages were analysed to investigate their possible role in the production of volatile compounds in nocturnal species *Nymphaea amazonum*, *N. gardneriana*, *N. prolifera* (*Nymphaea* subgenus *Hydrocallis*) and *Victoria cruziana*, and in diurnal species *N. caerulea* (*Nymphaea* subgenus *Brachyceras*). Carpellary appendages were studied using light microscopy and scanning and transmission electron microscopy from pre-anthesis to the second day of anthesis. Anatomical and ultrastructural features are characteristic of osmophores. In all species, the most frequent components in secretory cells are amyloplasts, lipid bodies, mitochondria, rough endoplasmic reticulum and elaioplasts. The epidermis and multilayered parenchyma accumulate abundant starch grains and lipophilic substances, both of which vanish during anthesis. Amorphous substances are deposited between the plasmalemma and the outer cell wall of epidermal cells, and are then released by cuticular diffusion. Odour production in carpellary appendages might be an ancient role of primary importance both in diurnal and nocturnal species that are pollinated by deceit. Olfactory and visual cues of small carpellary appendages in *Nymphaea* subgenus *Brachyceras* correspond to bee pollination, and large carpellary appendages in subgenus *Hydrocallis* and *Victoria* represent parallel functional specializations of the flowers to the attraction and reward for exclusive beetle pollination.

KEYWORDS: amyloplast – *Brachyceras* – histochemistry – *Hydrocallis* – lipophilic substances – pollination modes – scent glands.

INTRODUCTION

Nymphaeaceae comprise five genera and *c*. 64 species (Borsch, Löhne & Wiersema, 2008; Löhne, Wiersema & Borsch, 2009; Endress & Doyle, 2015) and are included in the aquatic order Nymphaeales, one of the early divergent lineages of angiosperms (APG IV, 2016). The flowers of Nymphaeaceae species are solitary, perfect, actinomorphic and protogynous; they have numerous perianth organs and stamens and a gynoecium consisting of five (or three) to 40 fused carpels forming a unique cupped stigmatic surface. In *Barclaya* Wall., *Victoria* Lindl. and *Nymphaea* L. in its traditional circumscription (Conard, 1905; Schneider & Williamson, 1993), each carpel develops a dorsal prolongation termed carpellary appendage or stylar process. Diversity in size, shape and colour of carpellary appendages occurs at lower systematic levels. They are short and ovate or cordate in *Barclaya*, short and triangular in *Nymphaea* subgenera *Brachyceras* (Casp.) Conard and *Nymphaea* and large, clavate or linear in *Nymphaea* subgenera *Hydrocallis* (Planch.) Conard and *Lotos* (DC.) Conard and in *Victoria* (Conard, 1905; Wiersema, 1987; La-ongsri, Trisonthi & Balslev, 2009). In evolutionary terms, a single origin of the carpellary appendages in the family has been suggested (Löhne

*Corresponding author. E-mail: lmelisa.zini@yahoo.com.ar

et al., 2009). However, phenotypic variation has been postulated to reflect selection pressures on floral traits resulting from interactions between flowers of Nymphaeaceae and different functional groups of pollinators. The most prominent carpellary appendages are found in night-blooming species of *Nymphaea* and *Victoria*, which are exclusively pollinated by beetles (Scarabaeidae, Cyclocephalini), whereas in day-blooming species with melittophilous or generalist floral syndromes, appendages are inconspicuous or absent (Schneider, 1982a; Wiersema, 1988; Williamson & Schneider, 1994; Les *et al.*, 1999; Borsch *et al.*, 2008; Löhne *et al.*, 2009). Large carpellary appendages have been associated with primary attraction and reward during beetle pollination. Scent production and nutritional function were suggested for carpellary appendages of *N. amazonum* Mart. & Zucc. (Prance, 1980) and heat production for those of *N. lotus* L. (Hirthe & Porembsky, 2003) and *Victoria* spp. (Lamprecht *et al.*, 2002; Seymour & Matthews, 2006). Conversely, no function was suggested for small appendages in species with diurnal anthesis.

Animal-pollinated flowers typically have scent glands (Vogel, 1990). In nocturnal species, however, scent is especially important when visual signals become inefficient and long-distance olfactory signals are needed to attract a pollinator (Proctor, Yeo & Lack, 1996; Dötterl *et al.*, 2012). In, species of Nymphaeaceae pollinated by beetles, flies or bees, scent can be emitted through the perianth organs, staminodes and connective appendages. These secretory structures were detected only via neutral red staining (Valla & Cirino, 1972; Hirthe & Porembsky, 2003; Zini, Galati & Ferrucci, 2017) or olfactory tests (Prance, 1980; Wiersema, 1987; Hirthe & Porembsky, 2003), but there are no records of anatomical or ultrastructural studies. Carpellary appendages have been proposed as possible sites of synthesis and release of volatile compounds (Prance, 1980; Hirthe & Porembsky, 2003). Here, the anatomy, histochemistry and ultrastructure of such appendages were investigated for the first time, under the hypothesis that prominent carpellary appendages of *Nymphaea* subgenus *Hydrocallis* and of *Victoria* would display morphological and anatomical differences, but would conserve functional aspects associated with a similar pollination mode, whereas small carpellary appendages of subgenus *Brachyceras* would reveal a lower degree of specialization. Finally, an overview on the distribution of these structures in Nymphaeaceae in relation to the proposed functions, phylogeny and pollination strategies is provided.

MATERIAL AND METHODS

Plant material

Investigated species were collected and vouchers were deposited at the Northeast Institute of Botany Herbarium (CTES), Corrientes, Argentina. Details are provided in Table 1.

Light microscopy (LM)

For anatomical characterization, the material was processed by dehydration through an ethanol series with a pre-impregnation rinsing with tertiary butyl alcohol (Gonzalez & Cristóbal, 1997) and infiltration in Histoplast paraffin (Biopack, Buenos Aires, Argentina), according to Johansen (1940). Flowers were sectioned transversely and longitudinally (12 µm thick) with a rotary microtome; the sections were stained with Astra blue–safranin (Luque, Sousa & Graus, 1996) and mounted in synthetic Canada balsam

Table 1. Taxa of *Nymphaea* and *Victoria* studied and voucher information

Genus/subgenus	Taxon	Voucher
Nymphaea subgenus *Hydrocallis* (night bloomers)		
	N. amazonum Mart. & Zucc. subsp. *pedersenii* Wiersema	Argentina, Province of Corrientes, *Zini et al. 17*
	N. gardneriana Planch.	*Zini et al. 10*.
	N. prolifera Wiersema	*Zini et al. 19*
Nymphaea subgenus *Brachyceras* (day bloomer)		
	N. caerulea Savigny	*Zini et al. 16*
Victoria (night bloomer)		
	V. cruziana Orb.	Argentina, Province of Chaco, *Zini et al. 18*

(Biopur, Buenos Aires, Argentina). In addition, carpel appendages of *N. caerulea*, *N. gardneriana*, *N. prolifera* and *V. cruziana* were pre-fixed in 1% glutaraldehyde, 4% formaldehyde in phosphate buffer (pH 7.2) for 2 h and were post-fixed in 1.5% OsO_4 at 2 °C in the same buffer for 3 h. Dehydration was made using ascending graded series of acetone. Samples were embedded in Spurr's resin and sectioned using a Reichert–Jung ultramicrotome. Sections of 1 µm were stained with toluidine blue.

For the histochemical characterization, living carpellary appendages in three stages (immediately prior to anthesis, first day of anthesis and second day of anthesis) were transversally hand-sectioned and subjected to the following tests: cresyl blue for detecting mucilage; eosin Y for proteins; $FeCl_3$ for phenolic compounds (Johansen, 1940); Lugol's reagent for starch grains (Johansen, 1940); Sudan IV for lipophilic substances (Johansen, 1940) and 0.1% xylidine Ponceau 2R for total proteins (Ruzin, 1999). For all tests the control samples were observed. Temporary slides were mounted in water-glycerine and were observed and photographed using a Leica DM LB2 compound microscope (Leica, Wetzlar, Germany), equipped with a digital camera.

Transmission electron microscopy (TEM)

For ultrastructural studies, samples in Spurr's resin were cut (70 nm thick) and stained with uranyl acetate and lead citrate (Zarlavsky, 2014). The ultrastructure was examined and photographed with a Phillips EM 301 TEM.

Scanning electron microscopy (SEM)

Fixed flowers were dissected and dehydrated through a series of increasing ethanol solutions. The carpellary appendages were then critical point-dried with solvent-substituted liquid carbon dioxide and coated with a thin layer of gold palladium. Photomicrographs were obtained using a JEOL 5800 LV at 20 kV (JEOL USA, Peabody, MA, USA).

Neutral red test

For each species, putative sites of fragrance production in carpellary appendages were analysed by submerging entire flowers in an aqueous solution of neutral red (1:10 000, Vogel, 1990) for one hour. The flowers were collected and tested in the afternoon of the first day of anthesis. Morphological traits were observed with a Leica MZ6 stereomicroscope.

RESULTS

Morphology

Nymphaea amazonum, *N. gardneriana*, *N. prolifera* and *Victoria cruziana* have a syncarpous gynoecium consisting of congenitally fused carpels. In *N. caerulea*, the carpels are congenitally fused only at their bases. The distal part of each carpel is elongated into an appendage. In all *Nymphaea* spp., carpellary appendages are free, whereas in *V. cruziana* the dorsal side is adnate to the inner staminodia and to the hypanthium (Fig. 1A–E). In the night-blooming species *N. gardneriana*, *N. prolifera*, *N. amazonum* and *V. cruziana*, the appendages are reddish, whereas in the day-blooming *N. caerulea* they are yellow (Fig. 1F–J). In *N. prolifera* and *N. amazonum*, multicellular uniseriate papillae resembling the stigmatic ones extend for a short distance on the appendage (Fig. 2A).

Appendages are clavate in *N. prolifera*, *N. amazonum*, and *V. cruziana,* linear in *N. gardneriana* and conical in *N. caerulea* (Figs 1A–J, 2A–C). *Victoria cruziana* and *N. caerulea* have the largest and shortest appendages, respectively. The principal morphological characters of the appendages are summarized in Table 2.

On the first day of anthesis (female phase), the appendages are extended, mostly hidden under the innermost tepals (Fig. 1A, B). On the second day of anthesis, when the flower is fully open (male phase), the appendages bend inwards and almost cover the stigmatic surface (Fig. 1C). This movement of carpellary appendages was not observed in *N. caerulea* or *V. cruziana*. In all species, fragrance is perceivable from pre-anthesis up to the second day of anthesis.

After immersion of the flowers in neutral red, scent-producing regions in carpellary appendages were difficult to locate. Although a diffuse reaction was observed in *N. gardneriana*, *N. prolifera*, *N. amazonum* and *V. cruziana*, the deep pigmentation of these appendages masked the stain (Fig. 1F–H, J). In *N. caerulea*, neutral red stained the tip of the carpellary appendage (Fig. 1I).

The cuticle is multipapillate in *Nymphaea* spp. and smooth to striate in *V. cruziana* (Fig. 2D–H). Stomata and hydropotes are present only in the appendages of *Nymphaea*, although the former are absent in *N. caerulea* (Fig. 2D, E). Each hydropote is four-celled. In SEM, deposits that resemble epicuticular waxes are rarely observed in *N. gardneriana*, *N. prolifera* and *N. amazonum* (Fig. 2D–F). The cuticle remains uninterrupted after anthesis; it is intact in all *Nymphaea* spp. and forms irregular swellings in *V. cruziana* (Fig. 2I).

Anatomy

Carpellary appendages are mostly aerenchymatic, with thick-walled cells in *N. prolifera, N. amazonum*

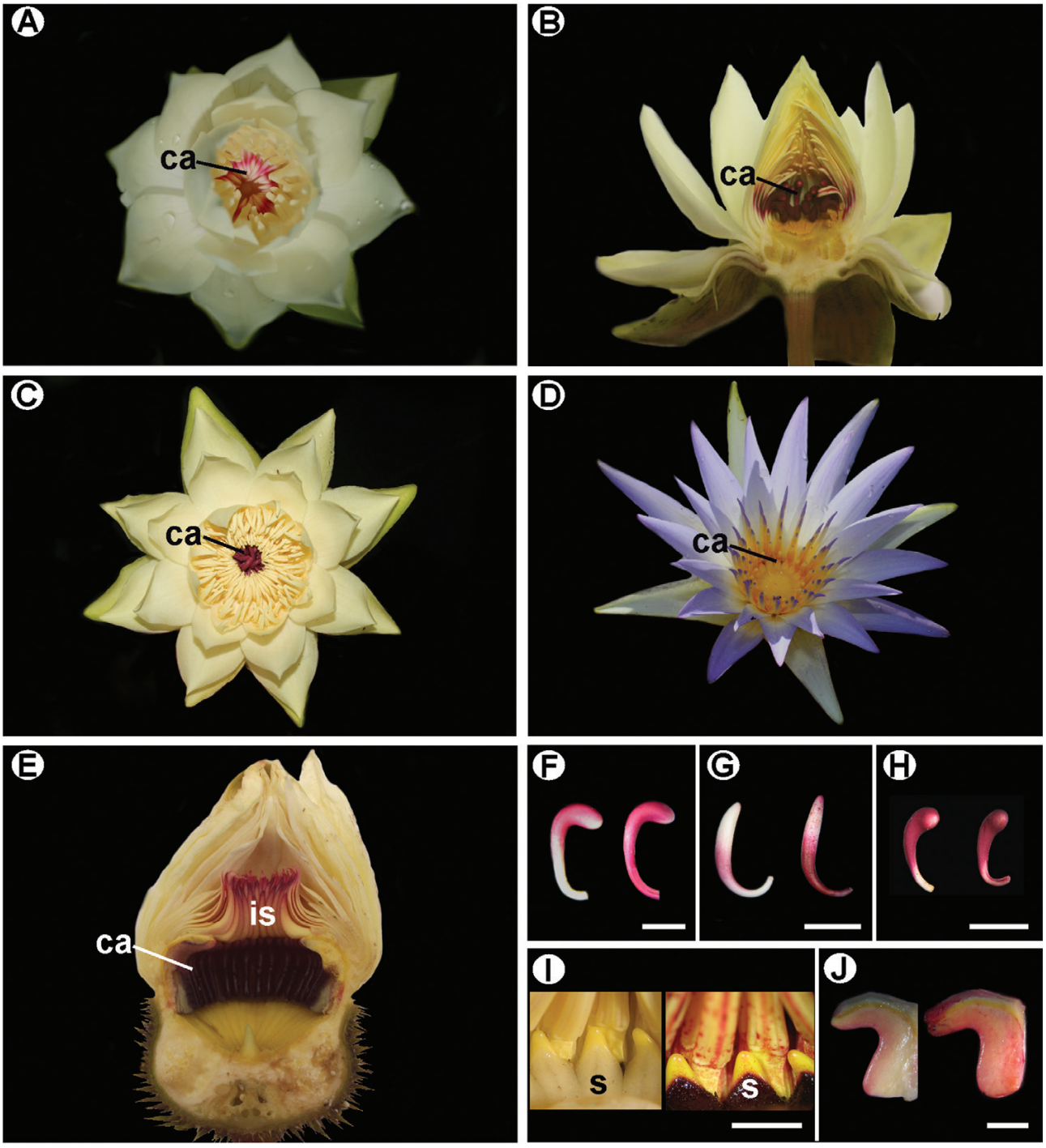

Figure 1. A–E, Location of carpellary appendages in the flower at anthesis in the studied species. A, *Nymphaea gardneriana*, male phase; B, longitudinal section of the flower of *N. prolifera* in female phase; C, *N. amazonum*, male phase with appendages covering the stigmatic cup; D, *N. caerulea*, diurnal species with short appendages; E, longitudinal section of the flower of *Victoria cruziana* in female phase and F–J, tests with neutral red, untreated (left) and treated (right) carpellary appendages. F, *N. amazonum*; G, *N. gardneriana*; H, *N. prolifera*; I, *N. caerulea* and J, *V. cruziana.* ca, carpellary appendage; is, inner staminodia; s, stigma. Scale bars = 5 mm (F–J).

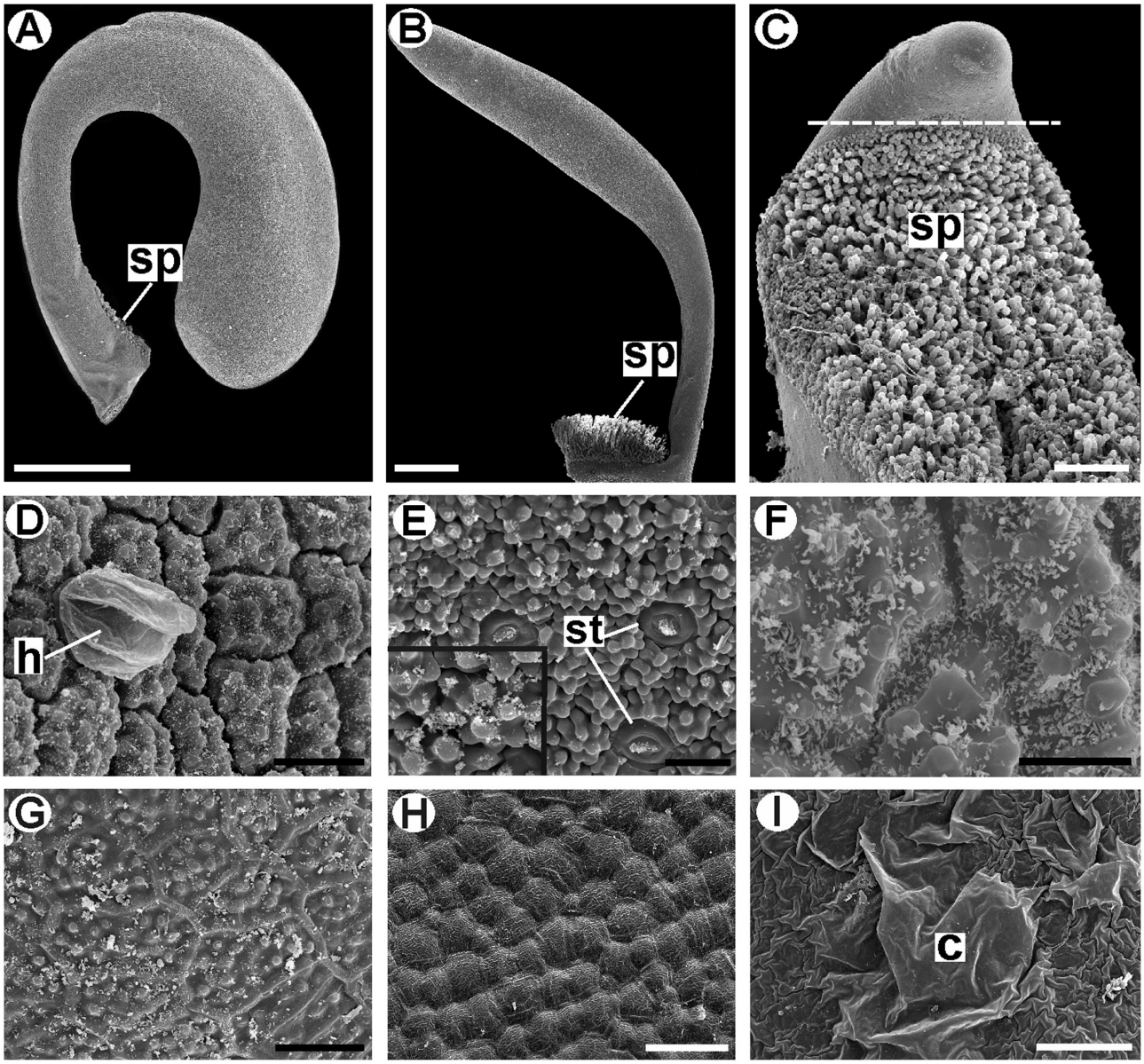

Figure 2. Micromophology of carpellary appendages. Scanning electron micrographs. A, *Nymphaea prolifera*; B, *N. gardneriana* and C, *N. caerulea*. Carpellary appendage boundary with dashed line; D, epidermis with a hydropote in *N. gardneriana*; E, epidermis with stomata in *N. prolifera*, inset showing wax-like deposits; F, detail of the wax-like deposits on epidermis of *N. amazonum*; G, multipapillate cuticle in *N. caerulea*; H, epidermal cells at the base of the appendage of *Victoria cruziana* and I, cuticular blisters at second day of anthesis in *V. cruziana*. c, cuticle; h, hydropote; sp, stigmatic papillae; st, stomata. Scale bars = 10 µm (E, F), 20 µm (D, G), 50 µm (H), 200 µm (C, I), 1 mm (A, B).

and *V. cruziana*, and well supplied with collateral vascular bundles (Fig. 3A–K). In transverse sections, epidermal cells are quadrangular or rectangular. The external periclinal wall may be slightly convex in *N. gardneriana*, *N. prolifera* and *N. amazonum* or flat in *N. caerulea* (Fig. 3G–J). Epidermal cells are radially elongated in *V. cruziana* and their external periclinal wall is notably thicker than in *Nymphaea* spp. (Fig. 3K–M). In post-anthetic stages, the cell wall becomes lax and cuticular blisters are formed, but the latter show no secretions (Fig. 3M). In the middle and at the apex of carpellary appendages, just before anthesis and during anthesis, parenchyma cells have secretory characteristics (dense cytoplasm, conspicuous nucleus and vacuoles of different sizes; Fig. 3A–G, I–K). In carpellary appendages of flowers on the second day of anthesis, these cells present a less dense cytoplasm and larger vacuoles than in previous stages (Fig. 3H,

Table 2. Comparison of principal morphological characters of the carpellary appendages of the studied species of *Nymphaea* and *Victoria*

	Night bloomers			Day bloomers	Night bloomer
	Nymphaea subgenus *Hydrochallis*			*Nymphaea* subgenus *Brachyceras*	*Victoria*
	N. amazonum	*N. gardneriana*	*N. prolifera*	*N. caerulea*	*V. cruziana*
Shape	clavate	linear	clavate	conical	clavate
Length	12–20 mm	10–15 mm	8–15 mm	1.5 mm	~30 mm
Colour	reddish	reddish	reddish	yellow	reddish
Cuticle	multipapillate	multipapillate	multipapillate	multipapillate	smooth to striate
Waxes	Yes	Yes	Yes	No	No
Stomata	Yes	Yes	Yes	No	No
Hydropotes	Yes	Yes	Yes	Yes	No

M). There are simple or branched acicular sclereids in *N. gardneriana* (base of the appendage) and *N. prolifera* (subepidermal), and astrosclereids in *V. cruziana* (Fig. 4A–C). Calcium oxalate crystals in the form of druses occur in *N. amazonum* and *N. caerulea*, and prismatic crystals occur in *N. gardneriana*, *N. prolifera* and *N. caerulea* (Figs 3G, 4D).

Histochemistry

Compound starch grains were observed in *N. gardneriana* under polarized light (Fig. 4E). Treatments with Lugol reagent revealed starch grains along the entire appendage of mature buds and open flowers in all five species (Fig. 4F–I). In *N. caerulea* and *N. gardneriana*, starch grains are concentrated at the apex of the appendage. Sudan IV stained the cuticle and lipid droplets within numerous cell layers in mature buds and open flowers of the five studied species (Fig. 5A–K). The lipid substances are especially abundant in the middle and apical regions of the carpellary appendages, but they are scarcer in epidermal cells because the central vacuole occupies most of the cytoplasm (Fig. 5A, G, I). The carpellary appendage of *N. gardneriana* at anthesis presents amorphous lipid substances (Fig. 5B). In *V. cruziana* there are lipid substances on the epidermis surface (Fig. 5K). After the first day of anthesis, the starch grains and lipids decrease both in the epidermis and underlying parenchyma. These substances continue to decrease or are almost absent after the second day of anthesis (Fig. 5C, F).

With light microscopy, proper epidermal cells and subsidiary cells of the stomata and hydropotes react positively with neutral red. The terminal cell of the hydropote may be lens-shaped or finger-like and deciduous; it reacts positively with cresyl blue and neutral red, revealing a mucilaginous substance (Fig. 6A, B). In *N. gardneriana*, the stain accumulates in the vacuoles and in *V. cruziana*, it mainly accumulates in the cytoplasm (Fig. 6B, C). The night-blooming species have anthocyanins in the epidermis vacuoles (Fig. 6E, F).

Ferric chloride stains polyphenols in epidermal cells of *N. gardneriana*, *N. prolifera* and *V. cruziana* and in idioblasts of the secretory parenchyma of *N. prolifera* and *V. cruziana*, even at pre-anthesis stage (Fig. 6D–F). As a unique feature, the upper boundary of the carpellary appendage of *V. cruziana* exhibits several phenolic cell layers stained with $FeCl_3$ at anthesis (Fig. 7A–C). In second-day flowers, phenolic cell layers become loose and separate into individual cells (Fig. 7C). Protein corpuscles are detected with eosin in some parenchyma cells of *N. prolifera* (Fig. 7D). Xylidine Ponceau stains the cytoplasm of parenchyma cells in *V. cruziana* (Fig. 7E).

Ultrastructural features

A similar ultrastructure is observed in the carpellary appendages of *N. caerulea*, *N. gardneriana* and *V. cruziana*. Immediately before anthesis, parenchymatous and epidermal cells appear metabolically active and in secretory phase. The cells exhibit a lobed nucleus and a dense cytoplasm occupied by numerous amyloplasts, lipid globules which usually coalesce, mitochondria with well-developed cristae, free ribosomes, abundant RER profiles and some dictyosomes with a few associated vesicles (Fig. 8A–F). Abundant plasmodesmata connecting parenchymal cells are observed, and the latter in turn connect with the epidermal cells (Fig. 8C). In epidermal cells, electron-dense and amorphous lipophilic substances between the plasmalemma and the outer cell wall are observed (Fig. 8F). On the first day of anthesis, the most notable cytological changes are the depletion of starch reserves occurring concomitantly with the accumulation of plastoglobuli in the stroma of the plastids and the reduction of lipid globules in the cytoplasm (Fig. 9A–F).

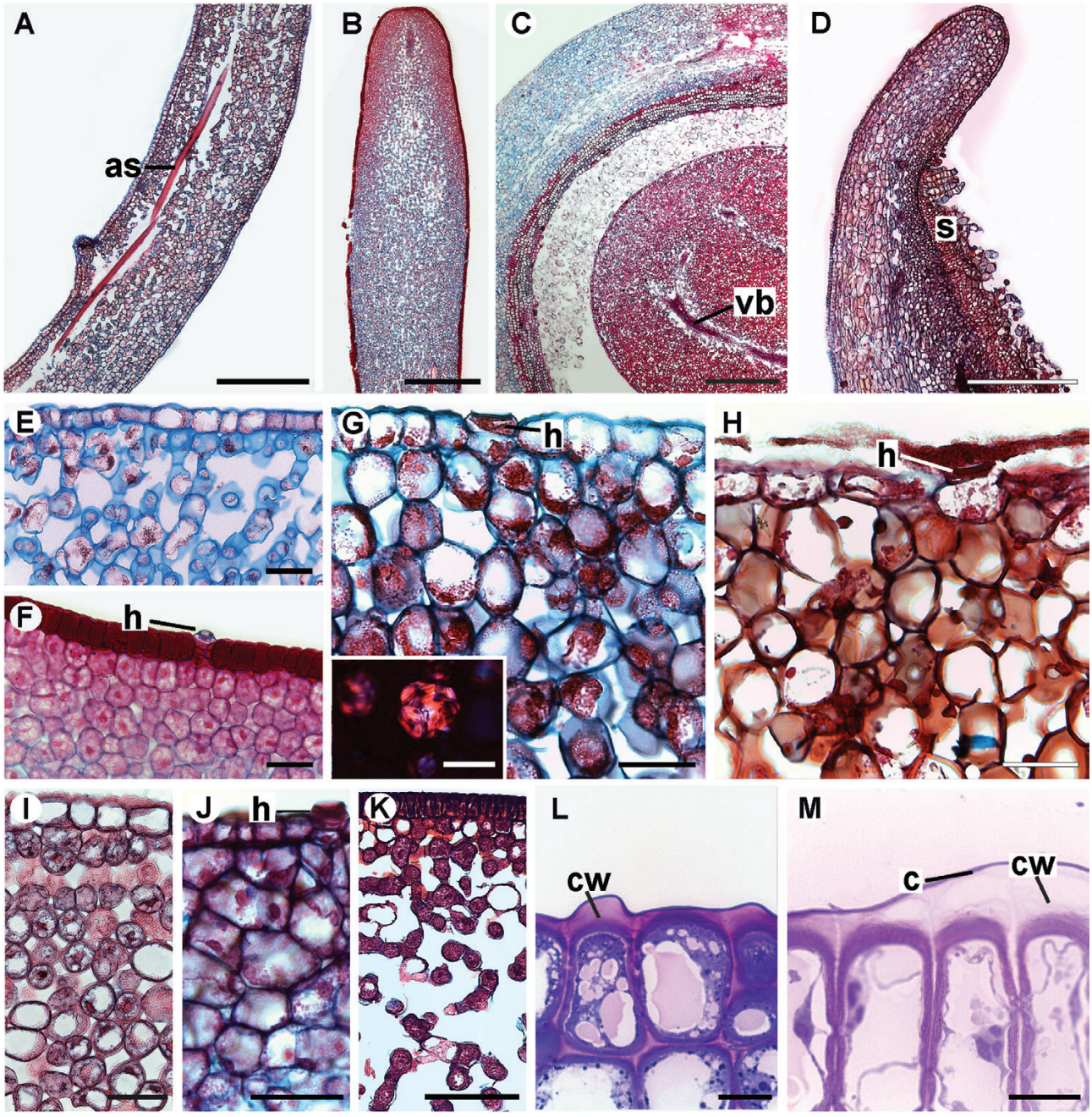

Figure 3. Anatomy of carpellary appendages with bright field microscope. A, B, longitudinal sections of basal and apical parts, respectively, just prior to the first day of anthesis in *Nymphaea gardneriana*; C, longitudinal section with part of the base and apex of the clavate appendage of *N. amazonum* at pre-anthesis; D, longitudinal section of carpellary appendage of *N. caerulea*; E, F, epidermis and parenchyma of the base and apex, respectively, in *N. gardneriana*; G, H, transverse sections of epidermis and parenchyma at first and second day of anthesis, respectively, in *N. gardneriana*; in G, inset with a druse under polarized light; I, longitudinal section of epidermis and parenchyma at anthesis of *N. prolifera*; J, epidermis and parenchyma at anthesis in *N. caerulea*; K, detail of transversal section of epidermis and parenchyma in pre-anthesis in *Victoria cruziana* and L, M, sections (1 µm) showing cuticle and epidermal cells in pre-anthesis and in second-day flowers, respectively, in *V. cruziana*. as, astrosclereid; c, cuticle; cw, cell wall; h, hydropote; s, stigma; vb, vascular bundle. Scale bars = 500 µm (A, B, C), 200 µm (D), 20 µm (G, H, L, M), 50 µm (E, F, I, J).

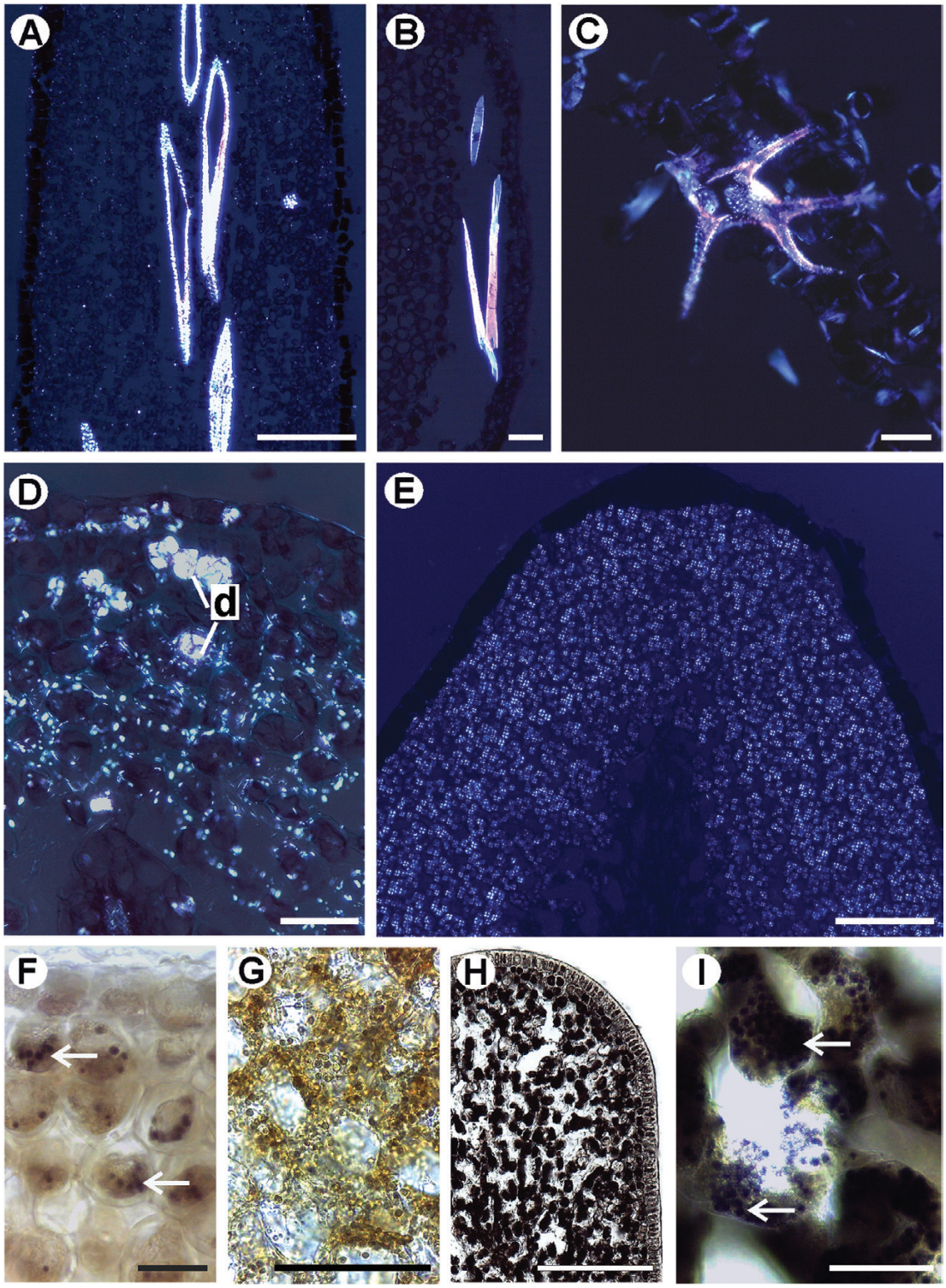

Figure 4. Anatomy and histochemical features of carpellary appendages. A–E, Polarized light. F–I, Lugol. A, acicular sclereids in *Nymphaea gardneriana*; B, subepidermal acicular sclereids in *N. prolifera*; C, astrosclereid in *Victoria cruziana*; D, druses and prismatic crystals in *N. caerulea*; E, starch grains at the apex at anthesis in *N. gardneriana*; F; parenchyma with starch grains (arrows) at anthesis in *N. amazonum*; G, Parenchyma of the apex with positive reaction to Lugol at anthesis in *N. caerulea*; H, transverse section of the apex stained with Lugol in *V. cruziana* and I, detail of starch grains (arrows) in *V. cruziana*. d, druse. Scale bars = 50 µm (A–D, F, G, I), 100 µm (E), 500 µm (H).

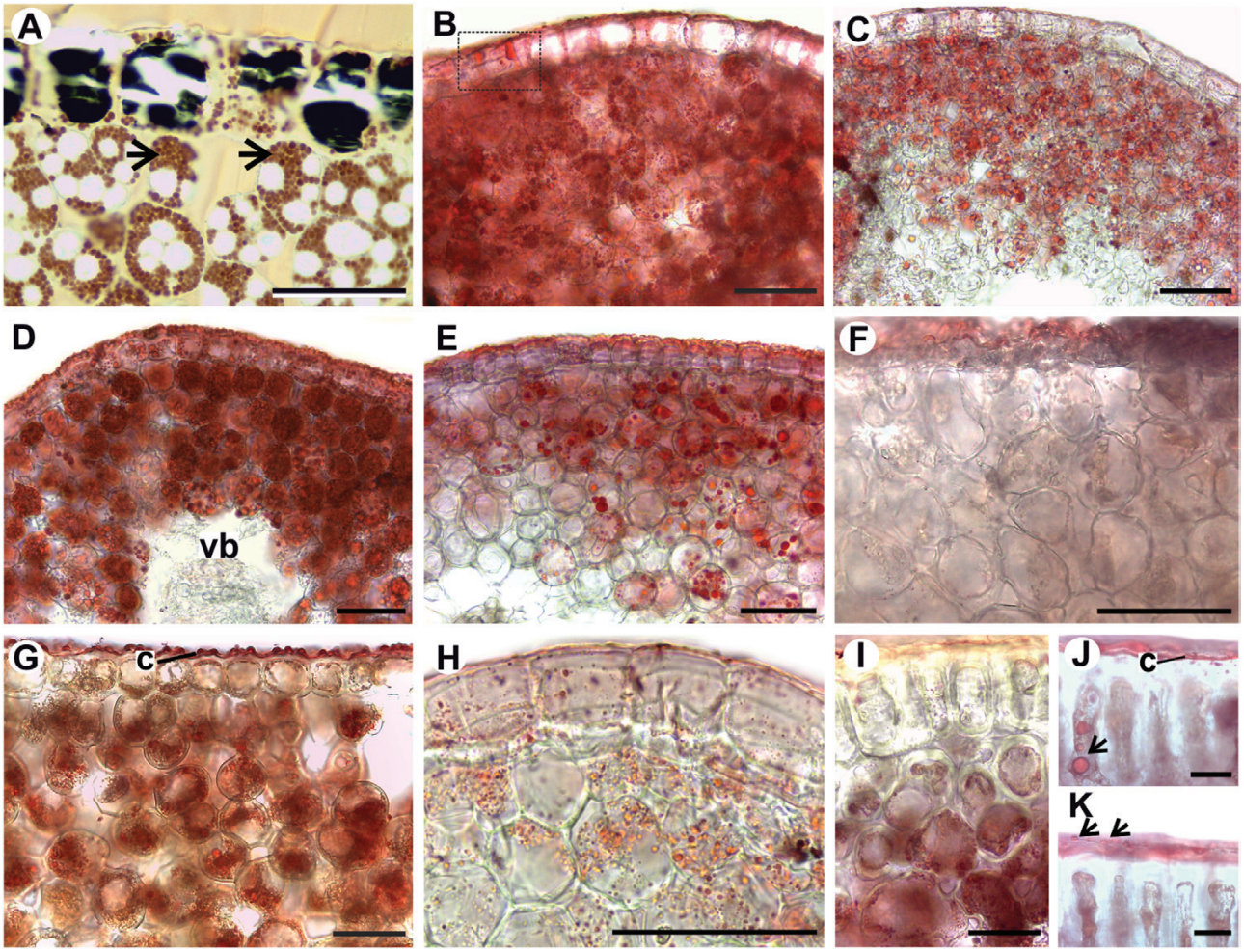

Figure 5. Histochemical features of carpellary appendages. A–K, Sudan IV. A, epidermis and parenchyma at pre-anthesis showing vacuoles with dark contents and positive reaction of lipid globules in section (1 µm) of *Nymphaea gardneriana* (arrows); B, epidermis and parenchyma cells filled with lipid droplets at first day of anthesis in *N. gardneriana*; amorphous substance is seen between the radial cell walls of epidermal cells (dashed rectangle); C, lipid droplets at second day of anthesis of *N. gardneriana*; D, epidermis and parenchyma with positive reaction to Sudan IV, except for the vascular bundle in *N. prolifera*; E, epidermis and parenchyma with weaker positive reaction to Sudan IV at second day of anthesis in the same species; F, tissue with negative reaction to Sudan IV after the second day of anthesis in *N. prolifera*; G, cuticle and parenchyma with positive reaction for lipophilic substances at first day of anthesis of *N. amazonum*; H, detail from the apex with positive reaction to Sudan IV at first day of anthesis in *N. caerulea*; I, transverse section of the apex on the first day of anthesis in *Victoria cruziana*; J, detail of epidermis showing the cuticle and lipid substances in the cell (arrow) in *V. cruziana* and K, lipid substances on the surface of the appendage (arrows) in *V. cruziana*. c, cuticle; vb, vascular bundle. Scale bars = 20 µm (A, J, K), 50 µm (B–I).

As at the pre-anthesis stage, numerous mitochondria and some dictyosomes are observed (Fig. 9E).

DISCUSSION

THE OSMOPHORE ROLE OF CARPELLARY APPENDAGES AND OTHER ASSIGNED FUNCTIONS

In this study, the anatomical, histochemical and ultrastructural features of the carpellary appendages in *Nymphaea* and *Victoria* provide evidence to link these peculiar structures with sites of scent emission. The exposed secretory structures in the floral organs specialized in the biosynthesis and emission of volatile attractants for pollinators were termed osmophores by Vogel (1963). These glands may be structured by a secretory cell layer and one or more layers of cells functionally related to synthesis and storage.

The neutral red test is traditionally used for macroscopical localization of scent-producing organs, although it is not specific for this type of secretory tissue

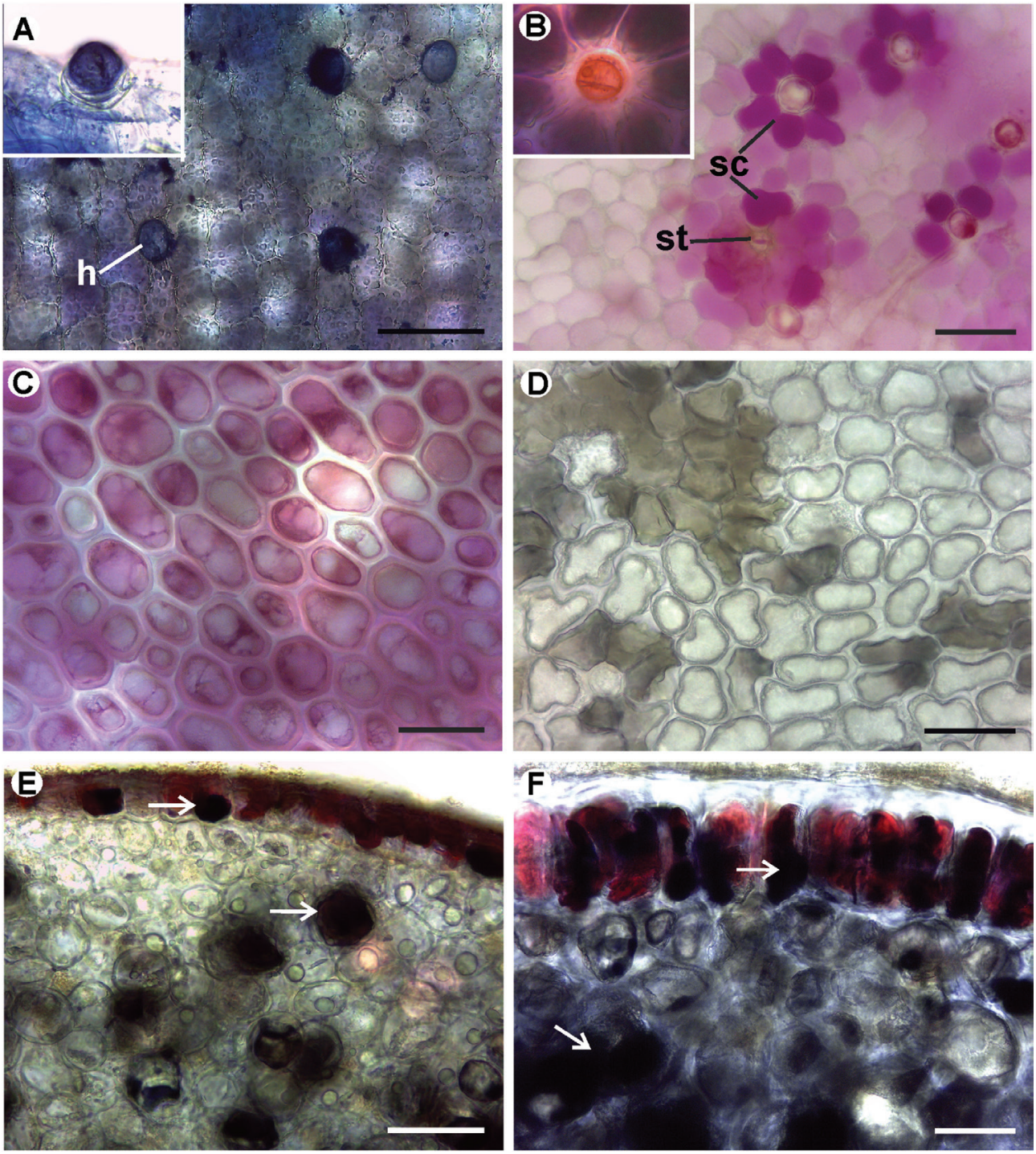

Figure 6. Histochemical features of carpellary appendages observed with bright field microscope. A, epidermis of *Nymphaea prolifera* stained with cresyl blue reveals mucilage in the terminal cell of the hydropote (inset); B, epidermis of *N. gardneriana* stained with neutral red; the terminal cell of the hydropote (inset) and some subsidiary cells stain; C, epidermis of *V. cruziana* stained with neutral red; D, surface view of epidermis with positive reaction to $FeCl_3$ for polyphenols in *N. gardneriana*; E, idioblasts with positive reaction to $FeCl_3$ in epidermis and parenchyma (arrows) at pre-anthesis in *N. prolifera* and F, epidermal and parenchyma cells with positive reaction to $FeCl_3$ (arrows) at anthesis in *V. cruziana*. Scale bars = 50 µm (A–F).

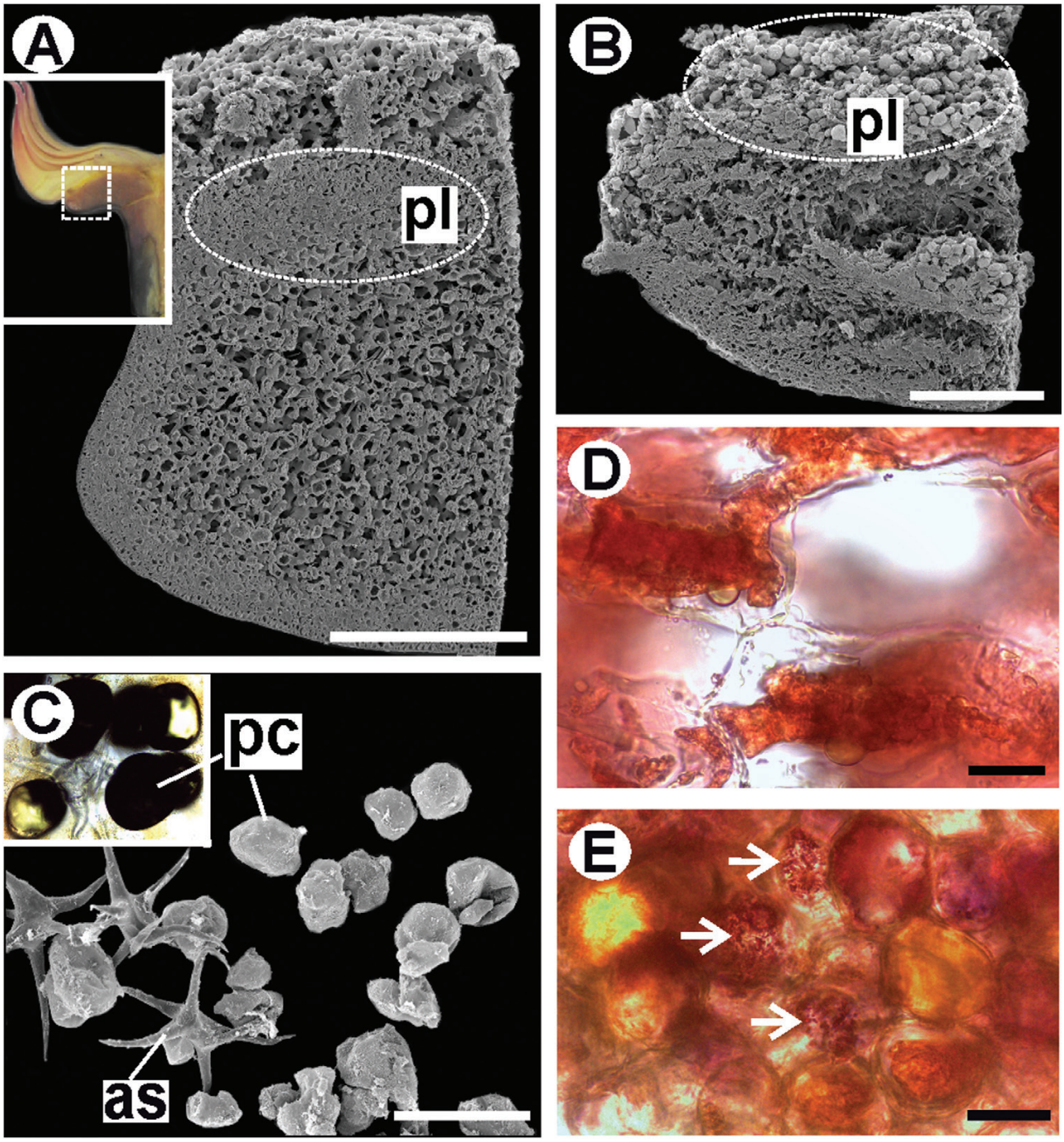

Figure 7. Scanning electron micrographs of *Victoria cruziana*. A–C, Histochemical features of carpellary appendages and D, E, under a bright field microscope. A, detail of longitudinal sections of the apex of the carpellary appendage at pre-anthesis; phenolic cell layers are indicated with dashed circle; B, phenolic cell layers at post-anthesis (dashed circle); C, the cells of this layer have positive result with $FeCl_3$ (inset); D, cytoplasm of secretory cells stained with xylidine Ponceau in *V. cruziana*; E, parenchyma cells stained with eosin reveal protein contents (arrows) at anthesis in *Nymphaea prolifera*. as, astrosclereid; pc, phenolic cells; pl, phenolic cell layers. Scale bars = 20 μm (D, E), 200 μm (C), 1 mm (A, B).

(Vogel, 1990; Weryszko-Chmielewska & Stpiczyńska, 1995; Effmert *et al.*, 2005; Amela García, Galati & Hoc, 2007). In the present study, this test was not efficient due to the natural deep red colour of the carpellary appendages in representatives of *Nymphaea* subgenus *Hydrocallis* and *Victoria*.

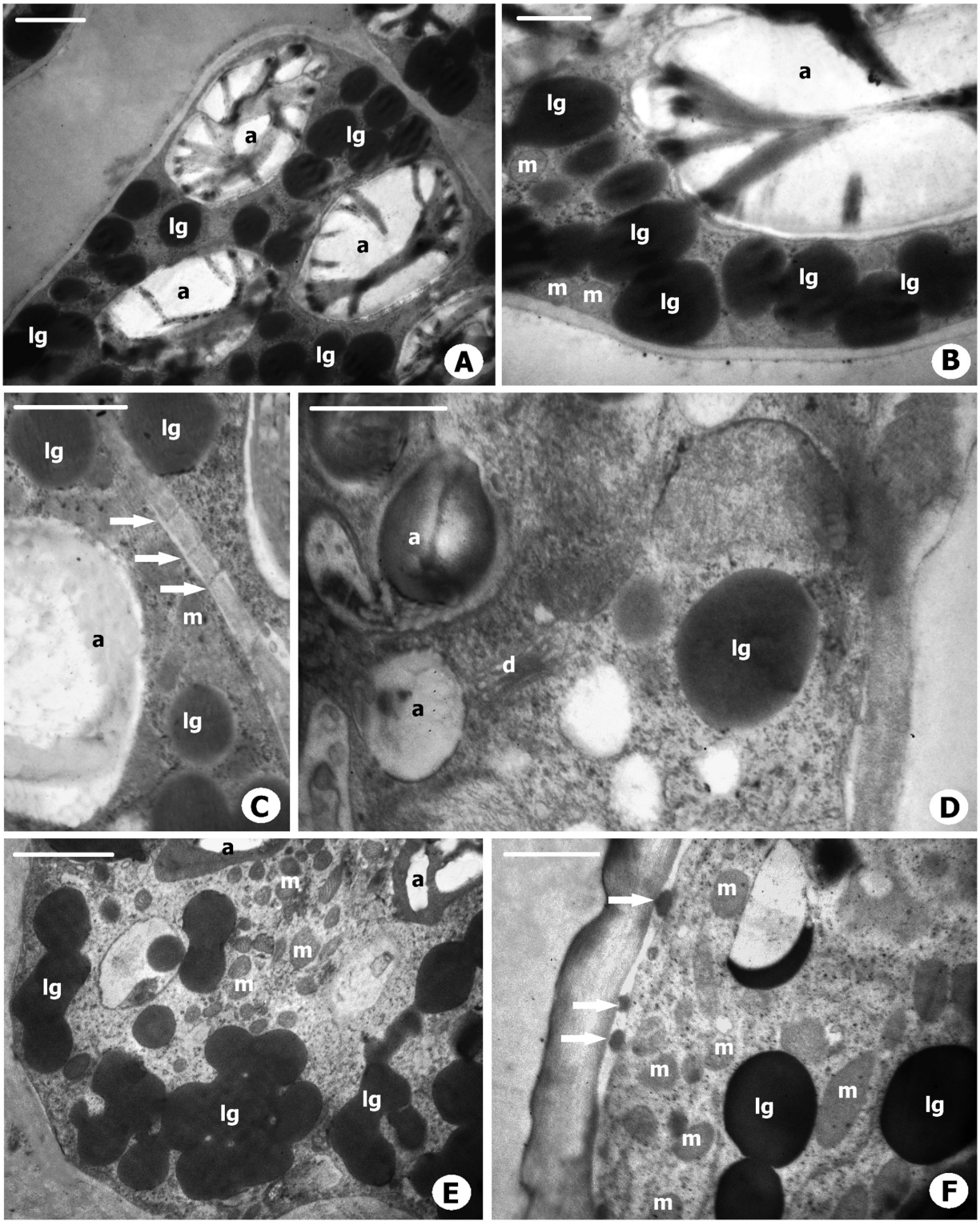

Figure 8. A–D, Ultrastructure of carpellary appendages in *Nymphaea gardneriana*, and E, *N. caerulea* and *Victoria cruziana* at pre-anthesis. A, Parenchyma cell filled with amyloplasts and lipid globules; B, detail of cytoplasm of A; C, detail of plasmodesmata between two parenchyma cells; D, detail of cytoplasm with a dictyosome; E, cytoplasm of parenchyma cell with coalescing lipid globules and numerous mitochondria and F, accumulation of electron-dense substances between the plasmalemma and cell wall (arrows) of epidermal cell. a, amyloplast; d, dictyosome; lg, lipid globule; m, mitochondrion. Scale bars = 1 μm (B, D); 2 μm (A, C, E, F).

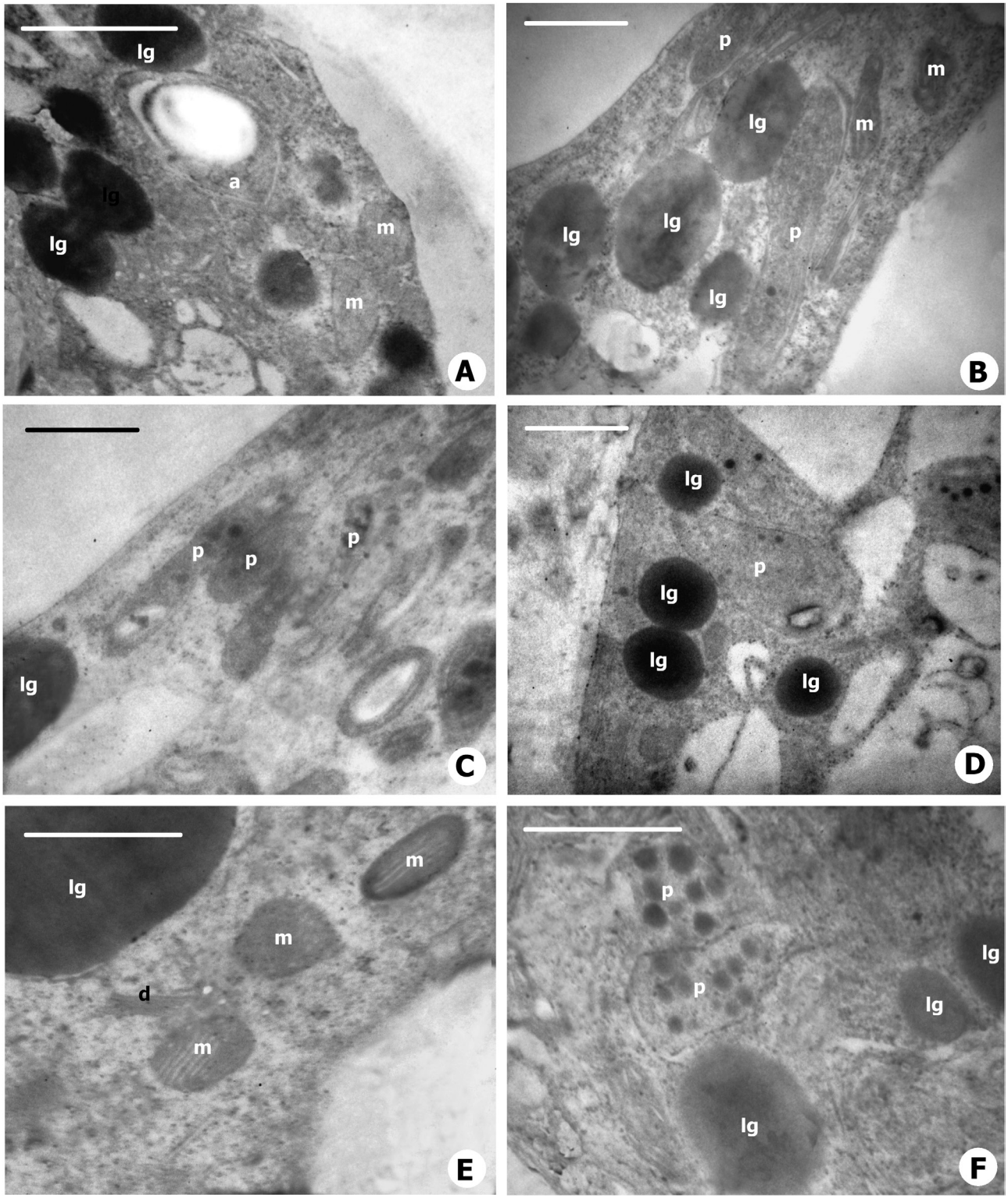

Figure 9. A–C, Ultrastructure of carpellary appendages of *Nymphaea gardneriana* and D–E, *N. caerulea* on the first day of anthesis. A, B, cytoplasm with predominance of lipid globules of different electron-densities and mitochondria; C, cytoplasm containing plastids devoid of starch grains but with osmiophilic globules; D, cytoplasm with lipid globules and plastids; E, detail showing mitochondria with well-developed cristae and dictyosome and F, detail of cytoplasm showing lipid globules and plastids with osmiophilic globules. a, amyloplast; d, dictyosome; lg, lipid globule; m, mitochondrion; p, plastid. Scale bars = 1 μm.

The parenchyma cells of the carpellary appendages have a large nucleus, dense cytoplasm predominantly with mitochondria, rough endoplasmic reticulum, dictyosomes in variable quantities and abundant plasmodesmata. These are all typical organelles of secretory cells (Fahn, 1988). Nevertheless, the most remarkable features of osmophores are the abundant starch reserves in the plastids, which are used during early anthesis, and lipophilic materials that disappear during the phases of fragrance emission, as in Apocynaceae, Araceae, Malphigiaceae, Orchidaceae and Passifloraceae (Vogel, 1990; Stpiczyńska, 1993, 2001; Buchen, 1998; Hadacek & Weber, 2002; Amela García *et al.*, 2007; Melo, Borba & Paiva, 2010). Other features here observed, associated with osmophores, are the presence of large intercellular spaces and a cytoplasm containing lipid droplets and elaioplasts (Pridgeon & Stern, 1983; Stern, Curry & Pridgeon, 1987; Curry *et al.*, 1988; Vogel, 1990; Stpiczyńska, 1993, 2001; Buchen, 1998; Melo *et al.*, 2010; Kowalkowska *et al.*, 2012; Sanguinetti *et al.*, 2012; Stpiczyńska & Davies, 2016; Marinho *et al.*, 2018; Wiśniewska *et al.*, 2018; Tölke *et al.*, 2019).

The lipophilic substances may be considered physical equivalents of the volatile compounds (Pridgeon & Stern, 1983; Stern *et al.*, 1987), and can be localized in different cellular compartments. In all *Nymphaea* spp. and in *V. cruziana*, lipid bodies are mainly scattered in the cytoplasm, as in osmophores of some species of Araceae, Orchidaceae, Passifloraceae and Apocynaceae (Vogel, 1990; Amela García *et al.*, 2007; Płachno, Świątek & Szymczak, 2010). Elaioplasts in the species studied here were detected after anthesis or at late anthesis, but there are cases in which these plastids prevail over other organelles in the active phase, e.g. in *Arum* L. (Araceae; Buchen, 1998), *Maxillaria polyphylla* Rchb.f. (Orchidaceae; Davies & Stpiczyńska, 2017), Fabaceae (Marinho *et al.*, 2018) and Apocynaceae (Tölke *et al.*, 2019). According to Dudareva *et al.* (2013), the most common ultrastructural feature of scent-producing organs is the presence of plastids, which are involved in the synthesis of volatile compounds, especially terpenoids, and in precursors of fatty acid derivatives and aromatics.

Aromatic substances or benzenoids are reported as constituents of volatile compounds involved in pollinator attraction (Jürgens, Webber & Gottsberger, 2000; Jürgens, Dötterl & Meve, 2006; Dötterl *et al.*, 2012; Leguet *et al.*, 2014; Kowalkowska *et al.*, 2018; Wiśniewska *et al.*, 2018). Similarly, aromatics are the dominant category of floral volatile compounds of *Nymphaea* and *Victoria*, followed by C5-branched chain esters and finally sesquiterpenes, which are reported for *Nymphaea* subgenus *Brachyceras* (Kite, Reynolds & Prance, 1991; Maia *et al.*, 2014). Despite variations in the composition of volatile compounds between diurnal and nocturnal species (reviewed in Maia *et al.*, 2014), no differences in the osmophores were detected at the ultrastructural level in this study.

Starch grains are considered the source of energy for the synthesis of fragrance or the secretory process, since they are quickly mobilized during active fragrance emission (Stern *et al.*, 1987; Vogel, 1990; Tölke *et al.*, 2019). However, the great abundance of amyloplasts associated with numerous mitochondria in carpellary appendages of the studied nocturnal species could also be related to the phenomenon of thermogenesis (Lamprecht *et al.*, 2002; Hirthe & Porembsky, 2003; Seymour & Matthews, 2006). Thermogenesis occurs as a consequence of the metabolic activity for massive synthesis and structural transformation of volatile compounds, and this may enhance the volatilization of fragrances when increases in temperature and scent emission are correlated (Vogel, 1990). In *Victoria amazonica* (Poepp.) Klotzsch, carpellary appendages produce 67% of the heat in the flower during the first night (Seymour & Matthews, 2006). Heat is an energetic reward during the visits of scarab beetles because it maintains their body temperatures (Seymour & Matthews, 2006). The dynamics of reserves of carpellary appendages in *Victoria* suggest that high secretory activity in the female phase may correspond with the high levels of thermogenesis to attract beetles and direct them towards the floral chamber. In contrast, the cell protoplast being poor in reserves in the male phase indicates that carpellary appendages are no longer effective in scent emission; similarly, Seymour & Matthews (2006) reported the cease of thermogenesis in that phase.

The epidermis of osmophores is most frequently composed of different types of papillae (Vogel, 1990; Stpiczyńska, 2001; Teixeira, Borba & Semir, 2004; Vogel & Hadacek, 2004; Ascensão *et al.*, 2005; Amela García *et al.*, 2007; Melo *et al.*, 2010; Gonçalves-Souza *et al.*, 2017). However, rounded epidermal cells or flat cells with cuticular ridges as in the studied species were also previously described (Stern *et al.*, 1987; Vogel, 1990; Ascensão *et al.*, 2005; Marinho *et al.*, 2014, 2018). In *Nymphaea* and *Victoria*, the epidermis is involved in the emission process and in the storage of materials. The same phenomenon occurs in osmophores of *Ceropegia* L. (Apocynaceae, Vogel, 1990), *Ophrys* L. (Orchidaceae, Vogel, 1990; Ascensão *et al.*, 2005), *Passiflora* L. (Passifloraceae, Amela García *et al.*, 2007) and some species of Fabaceae (Marinho *et al.*, 2014). The release of fragrance substances outside the gland usually occurs through microchannels in the cuticle (e.g. Apocynaceae, Płachno *et al.*, 2010; Orchidaceae, Stern *et al.*, 1987; Kowalkowska *et al.*, 2012; Kowalkowska, Kozieradzka-Kiszkurno & Turzyński, 2015; Sanguinetti *et al.*, 2012; Passifloraceae, Amela García *et al.*, 2007), by rupture of the cuticle or through pores present in the

cuticle (Orchidaceae: *Restrepia* Kunth, Pridgeon & Stern, 1983; *Gymnadenia* R.Br., Stpiczyńska, 2001; Apocynaceae: *Boucerosia* Wight & Arn., Płachno *et al.*, 2010), and in a few cases through stomata (Araceae: *Philodendron* Schott, Gonçalves-Souza *et al.*, 2017; Orchidaceae: *Acianthera* Scheidw., Melo *et al.*, 2010). Stomata were observed in carpellary appendages of *N. amazonum*, *N. gardneriana* and *N. prolifera*, but there is not enough evidence to confirm their role in the transport of volatile substances. All studied species exhibited both relatively thin cuticle areas and an outer cell wall with loosely arranged cellulose microfibrils. Cuticle thickness and ultrastructure may not be involved in permeability, but chemical composition is involved (Caissard *et al.*, 2004). Volatile compounds of low molecular weight may be able to diffuse through the microfibrils and the cutin due to their lipophilic nature (Tölke *et al.*, 2019); therefore, this is the plausible route of release of such substances from carpellary appendages. In *N. gardneriana*, electron-dense corpuscles observed in the cuticular layer suggest this release route. On the other hand, a rapid volatilization would be enhanced by the thermogenic property, preventing massive accumulation of exudates on the epidermal surface of these structures.

In addition to the osmophore and thermogenic functions of carpellary appendages in night-blooming species of *Nymphaea* and *Victoria*, the role as food reward for scarab beetles during the pollination event was recorded (Prance & Arias, 1975; Schneider, 1979; Hirthe & Porembski, 2003; Seymour & Matthews, 2006). In the studied populations, no signs of feeding were observed. Moreover, carbohydrates are consumed before anthesis and lipids are less abundant during anthesis. In the night-blooming species (*Nymphaea* subgenus *Hydrochallis* and *Victoria*), polyphenolic substances are accumulated in vacuoles of epidermal cells and idioblasts of the parenchyma at anthesis. These substances are considered to protect different organs against pathogen infections, UV radiations and herbivory (Castro & Demarco, 2008). Therefore, these appendages should not be compared with other plant tissues that provide food reward for insects (e.g. O'Dowd, 1980).

Forms and functions of carpellary appendages in relation to pollination modes

Selective pressures exerted by functional groups of similar pollinators are a prevalent underlying feature of floral diversification and convergent specialization (Fenster *et al.*, 2004). Thus, the overall morphological and functional shifts of the carpellary appendages can be understood as a response to shifts between functional groups of pollinators (Schneider, 1982a; Wiersema, 1988; Williamson & Schneider, 1994) in a current phylogenetic framework (Fig. 10). However, the morpho-anatomical organization of the carpellary appendages may be also important in revealing phylogenetic relationships at different hierarchical levels. This assumption is supported by the strong similarities between two closely related species, *N. amazonum* and *N. prolifera*, and especially by the multipapillate epidermal cell morphology, which is a phylogenetic signal for common ancestry of the clade comprising *Nymphaea* subgenera *Hydrocallis*, *Lotos*, *Anecphya* and *Brachyceras* (Zini *et al.*, 2017; Coiro & Barona Lumaga, 2018).

In Nymphaeaceae, pollination by deceit is an ancient strategy to increase fitness by cross-pollination. It consists of a combination of odour, heat, and coloured tepals to attract and trap insects in the female phase, when no direct reward is produced. Although bees are major pollinators in the family, the exclusive pollination by beetles in *Nymphaea* subgenera *Hydrocallis* and *Lotos* and in *Victoria* is of secondary derivation (reviewed by Thien *et al.*, 2009; Endress, 2010). *Barclaya*, *Euryale* Salisb. and *Nymphaea* subgenera *Anecphya*, *Brachyceras* and *Nymphaea* have species of diurnal anthesis. In these species, bees, beetles and flies are attracted to bright-coloured (blue, purple, red, violet, white, yellow) and fragrant flowers that do not produce heat (Conard, 1905; Okada & Otaya, 1930; Meeuse & Schneider, 1979; Schneider & Chaney, 1981; Schneider, 1982a,b; Capperino & Schneider, 1985). According to Löhne *et al.* (2009), carpellary appendages evolved once in the common ancestor of *Barclaya*, *Nymphaea s.l.*, *Euryale* and *Victoria*, and although this character is retained in most species, it is lost independently in derived lineages of the family. The absence of carpellary appendages is in correspondence with cleistogamy in *Euryale* and bee pollination in *Nymphaea* subgenus *Anecphya*, together with the evolution of a nectariferous floral apex in the latter (e.g. *N. ondinea* Löhne, Wiersema & Borsch, Schneider, 1983). Based on our findings, carpellary appendages in *N. caerulea* contribute to olfactory and visual cues, which are compatible with pollination by Hymenoptera. Similarly, the prominent carpellary appendages of *N. amazonum*, *N. gardneriana, N. prolifera* and *V. cruziana* are related to the provision of chemical and visual cues for scarab beetles. Furthermore, novel functions such as food and energetic rewards for *Nymphaea* subgenus *Lotos* have also been suggested (Hirthe & Porembsky, 2003).

Finally, scent production might be an ancient role of carpellary appendages of primary importance in the mechanism of pollination by deceit in both diurnal and nocturnal species. The evolutionary shifts into large structures in *Victoria* and the *Nymphaea* subgenus *Hydrocallis* + subgenus *Lotos* clade is here considered as parallel functional specializations to pronounced scent and heat production in response to the exclusive beetle pollination. The flower architecture

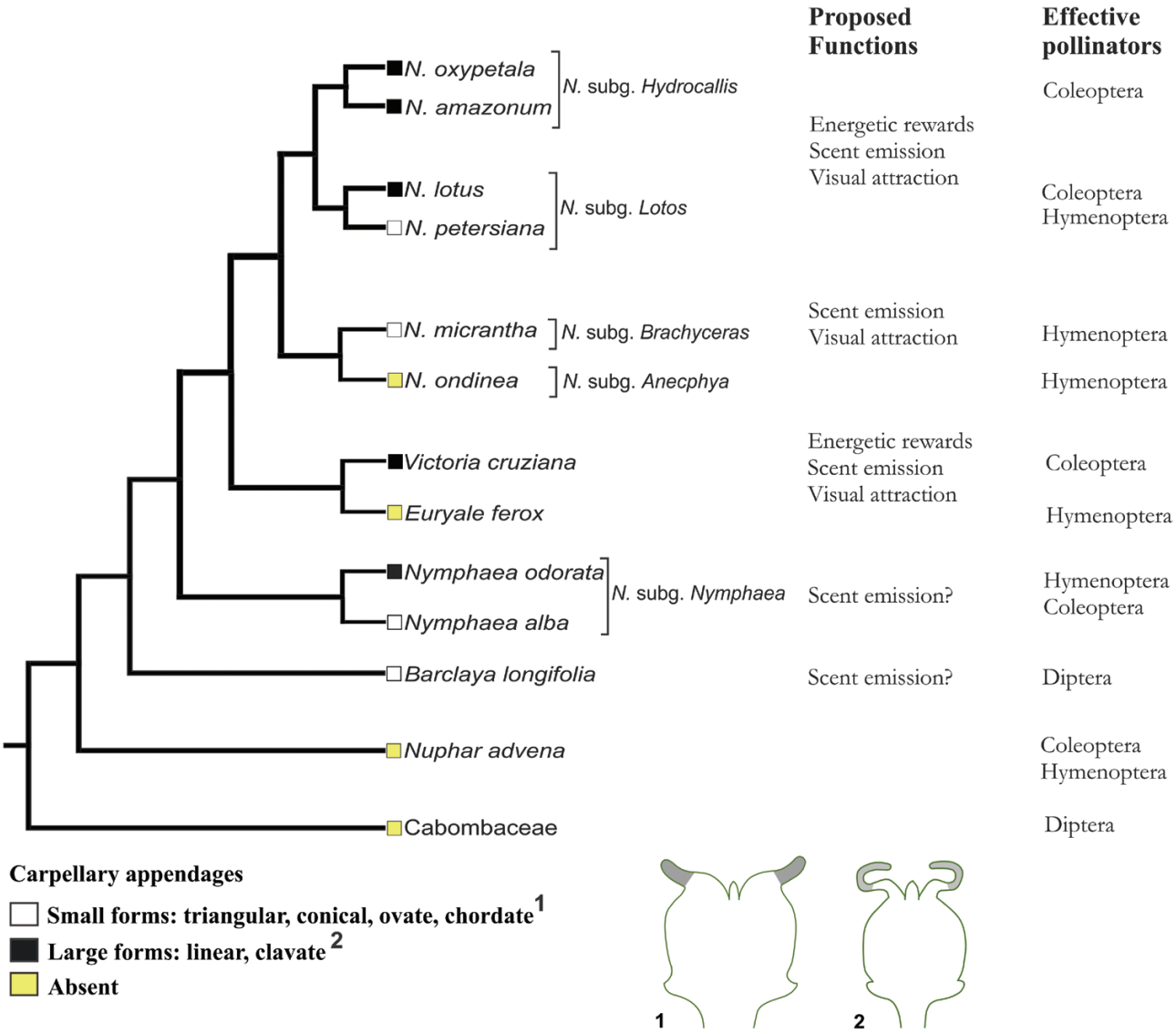

Figure 10. Morphologies of carpellary appendages mapped onto the phylogenetic tree for Nymphaeaceae. The topology is a combined molecular phylogenetic tree modified from Borsch *et al.* (2008) in which *Nymphaea* is paraphyletic, with *Nymphaea* subgenus *Nymphaea* sister to a clade comprising the other four subgenera and the *Euryale–Victoria* clade. For practical purposes, the appendages are classified in the categories large and small (if they are well-developed as to cover entire stigmatic surface or not), respectively. Information on pollination biology of Cabombaceae (outgroup) was obtained from Schneider & Jeter (1982) and that on the floral morphology of *Nymphaea* spp. from Conard (1905). See discussion for interpretations.

with distinctive low synorganization of its organs (Endress, 2006) might also have greatly favoured the morphological diversification of carpellary appendages among species of Nymphaeaceae.

ACKNOWLEDGEMENTS

This research was financially supported by grants from the Agencia Nacional de Promoción Científica y Tecnológica (PICT, FONCyT 2016-1160), the Universidad Nacional del Nordeste (PI number 15-A002), and the Universidad de Buenos Aires (UBACyT 20020160100012BA).

REFERENCES

Amela García MT, Galati BG, Hoc PS. 2007. Ultrastructure of the corona of scented and scentless flowers of *Passiflora* spp. (Passifloraceae). *Flora-Morphology, Distribution, Functional Ecology of Plants* **202:** 302–315.

APG IV. 2016. An update of the Angiosperm Phylogeny Group classification for the orders and families of flowering plants: APG IV. *Botanical Journal of Linnean Society* **181:** 1–20.

Ascensão L, Francisco A, Cotrim H, Pais MS. 2005. Comparative structure of the labellum in *Ophrys fusca* and *O. lutea* (Orchidaceae). *American Journal of Botany* **92:** 1059–1067.

Borsch T, Löhne C, Wiersema JW. 2008. Phylogeny and evolutionary patterns in Nymphaeales: integrating genes, genomes and morphology. *Taxon* **57:** 1052–1081.

Buchen B. 1998. Ultrastructure of the spadix-appendix cells during anthesis. In: Wilhelm B, Wolfram L, eds. Amorphophallus titanum. Stuttgart: Akademie der Wissenschaften und der Literatur; Mainz: Franz Steiner Verlag, 167–187.

Caissard JC, Joly C, Bergougnoux V, Hugueney P, Mauriat M, Baudino S. 2004. Secretion mechanisms of volatile organic compounds in specialized cells of aromatic plants. *Recent Research Developments in Cell Biology* **2:** 1–15.

Capperino ME, Schneider EL. 1985. Floral biology of *Nymphaea mexicana* Zucc. (Nymphaeaceae). *Aquatic Botany* **23:** 83–93.

Castro MD, Demarco D. 2008. Phenolic compounds produced by secretory structures in plants: a brief review. *Natural Product Communications* **8:** 1273–1284.

Coiro M, Barone Lumaga MR. 2018. Disentangling historical signal and pollinator selection on the micromorphology of flowers: an example from the floral epidermis of the Nymphaeaceae. *Plant Biology* **20:** 902–915.

Conard HS. 1905. *The waterlilies: a monograph of the genus* Nymphaea. Washington: Carnegie Institution of Washington.

Curry KJ. 1988. Osmophore development in *Stanhopea anfracta* and *S. pulla* (Orchidaceae). *Lindleyana* **3:** 212–220.

Davies KL, Stpiczyńska M. 2017. Comparative floral micromorphology and the ultrastructural basis of fragrance production in pseudocopulatory *Mormolyca s.s.* and non-pseudocopulatory *Maxillaria* section *Rufescens s.s.* (Orchidaceae). *Botanical Journal of the Linnean Society* **185:** 81–112.

Dötterl S, David A, Boland W, Silberbauer-Gottsberger I, Gottsberger G. 2012. Evidence for behavioral attractiveness of methoxylated aromatics in a dynastid scarab beetle-pollinated Araceae. *Journal of Chemical Ecology* **38:** 1539–1543.

Dudareva N, Klempien A, Muhlemann JK, Kaplan I. 2013. Biosynthesis, function and metabolic engineering of plant volatile organic compounds. *New Phytologist* **198:** 16–32.

Effmert U, Große J, Röse US, Ehrig F, Kägi R, Piechulla B. 2005. Volatile composition, emission pattern, and localization of floral scent emission in *Mirabilis jalapa* (Nyctaginaceae). *American Journal of Botany* **92:** 2–12.

Endress PK. 2006. Angiosperm floral evolution: morphological developmental framework. *Advances in Botanical Research* **44:** 1–61.

Endress PK. 2010. The evolution of floral biology in basal angiosperms. *Philosophical Transactions of the Royal Society B: Biological Sciences* **365:** 411–421.

Endress PK, Doyle JA. 2015. Ancestral traits and specializations in the flowers of the basal grade of living angiosperms. *Taxon* **64:** 1093–1116.

Fahn A. 1988. Secretory tissues in vascular plants. *New Phytologist* **108:** 229–257.

Fenster CB, Armbruster WS, Wilson P, Dudash MR, Thomson JD. 2004. Pollination syndromes and floral specialization. *Annual Review of Ecology, Evolution and Systematics* **35:** 375–403.

Gonçalves-Souza P, Schlindwein C, Dötterl S, Paiva EAS. 2017. Unveiling the osmophores of *Philodendron adamantinum* (Araceae) as a means to understanding interactions with pollinators. *Annals of Botany* **119:** 533–543.

Gonzalez AM, Cristóbal CL. 1997. Anatomía y ontogenia de semillas de *Helicteres lhotzkyana* (Sterculiaceae). *Bonplandia* **9:** 287–294.

Hadacek F, Weber M. 2002. Club-shaped organs as additional osmophores within the *Sauromatum* inflorescence: odour analysis, ultrastructural changes and pollination aspects. *Plant Biology* **4:** 367–383.

Hirthe G, Porembski S. 2003. Pollination of *Nymphaea lotus* (Nymphaeaceae) by rhinoceros beetles and bees in the northeastern Ivory Coast. *Plant Biology* **5:** 670–676.

Johansen DA. 1940. *Plant microtechnique.* New York: McGraw-Hill Book Company, Inc.

Jürgens A, Dötterl S, Meve U. 2006. The chemical nature of fetid floral odours in stapeliads (Apocynaceae – Asclepiadoideae – Ceropegieae). *New Phytologist* **172:** 452–468.

Jürgens A, Webber AC, Gottsberger G. 2000. Floral scent compounds of Amazonian Annonaceae species pollinated by small beetles and thrips. *Phytochemistry* **55:** 551–558.

Kite G, Reynolds T, Prance GT. 1991. Potential pollinator-attracting chemicals from *Victoria* (Nymphaeaceae). *Biochemical Systematics and Ecology* **19:** 535–539.

Kowalkowska AK, Kozieradzka-Kiszkurno M, Turzyński S. 2015. Morphological, histological and ultrastructural features of osmophores and nectary of *Bulbophyllum wendlandianum* (Kraenzl.) Dammer (*B.* section *Cirrhopetalum* Lindl., Bulbophyllinae Schltr., Orchidaceae). *Plant Systematics and Evolution* **301:** 609–622.

Kowalkowska AK, Margońska HB, Kozieradzka-Kiszkurno M, Bohdanowicz J. 2012. Studies on the ultrastructure of a three-spurred *fumeauxiana* form of *Anacamptis pyramidalis*. *Plant Systematics and Evolution* **298:** 1025–1035.

Kowalkowska AK, Pawłowicz M, Guzanek P, Krawczyńska AT. 2018. Floral nectary and osmophore of *Epipactis helleborine* (L.) Crantz (Orchidaceae). *Protoplasma* **255:** 1811–1825.

Lamprecht I, Schmolz E, Blanco L, Romero CM. 2002. Energy metabolism of the thermogenic tropical water lily, *Victoria cruziana*. *Thermochimica Acta* **394:** 191–204.

La-ongsri W, Trisonthi C, Balslev H. 2009. A synopsis of Thai Nymphaeaceae. *Nordic Journal of Botany* **27:** 97–114.

Leguet A, Gibernau M, Shintu L, Caldarelli S, Moja S, Baudino S, Caissard JC. 2014. Evidence for early intracellular accumulation of volatile compounds during spadix development in *Arum italicum* L. and preliminary data on some tropical aroids. *Naturwissenschaften* **101:** 623–635.

Les DH, Schneider EL, Padgett DJ, Soltis PS, Soltis DE, Zanis M. 1999. Phylogeny, classification and floral evolution

of water lilies (Nymphaeaceae; Nymphaeales): a synthesis of non-molecular, *rbcL*, *matK*, and 18S rDNA data. *Systematic Botany* **24:** 28–46.

Löhne C, **Wiersema JH**, **Borsch T. 2009.** The unusual *Ondinea*, actually just another Australian water-lily of *Nymphaea* subg. *Anecphya* (Nymphaeaceae). *Willdenowia* **39:** 55–59.

Luque R, **Sousa HC**, **Graus JE. 1996.** Métodos de coloracão de Roeser (1972) modificado Kropp E, 1972. Visando a substituicão do azul de astra por azul de alcião 8GS ou 8GX. *Acta Botanica Brasilica* **10:** 199–212.

Maia ACD, **de Lima CT**, **Navarro DMDAF**, **Chartier M**, **Giulietti AM**, **Machado IC. 2014.** The floral scents of *Nymphaea* subg. *Hydrocallis* (Nymphaeaceae), the New World night-blooming water lilies, and their relation with putative pollinators. *Phytochemistry* **103:** 67–75.

Marinho CR, **Martucci MEP**, **Gobbo-Neto L**, **Teixeira S. 2018.** Chemical composition and secretion biology of the floral bouquet in legume trees (Fabaceae). *Botanical Journal of the Linnean Society* **187:** 5–25.

Marinho CR, **Souza CD**, **Barros TC**, **Teixeira SP. 2014.** Scent glands in legume flowers. *Plant Biology* **16:** 215–226.

Meeuse BJ, **Schneider EL. 1979.** *Nymphaea* revisited: a preliminary communication. *Israel Journal of Plant Sciences* **28:** 65–79.

Melo DMC, **Borba EL**, **Paiva EAS. 2010.** Morphological and histological characterization of the osmophores and nectaries of four species of *Acianthera* (Orchidaceae: Pleurothallidinae). *Plant Systematics and Evolution* **286:** 141–151.

O'Dowd DJ. 1980. Pearl bodies of a Neotropical tree, *Ochroma pyramidale*: ecological implications. *American Journal of Botany* **67:** 543–549.

Okada Y, **Otaya T. 1930.** Study of *Euryale ferox* Salisb. VI. Cleistogamous versus chasmogamous flowers. *Shokubutsugaku Zasshi* **44:** 369–373.

Płachno BJ, **Świątek P**, **Szymczak G. 2010.** Can a stench be beautiful?–Osmophores in stem-succulent stapeliads (Apocynaceae-Asclepiadoideae-Ceropegieae-Stapeliinae). *Flora-Morphology, Distribution, Functional Ecology of Plants* **205:** 101–105.

Prance GT. 1980. A note on the pollination of *Nymphaea amazonum* Mart. & Zucc. (Nymphaeaceae). *Brittonia* **32:** 505–507.

Prance GT, **Arias JR. 1975.** A study of the floral biology of *Victoria amazonica* (Poepp.) Sowerby (Nymphaeaceae). *Acta Amazonica* **5:** 109–139.

Pridgeon AM, **Stern WL. 1983.** Ultrastructure of osmophores in *Restrepia* (Orchidaceae). *American Journal of Botany* **70:** 1233–1243.

Proctor M, **Yeo P**, **Lack A. 1996.** *The natural history of pollination.* New York: HarperCollins Publishers.

Ruzin SE. 1999. *Plant microtechnique and microscopy.* New York: Oxford University Press.

Sanguinetti A, **Buzatto CR**, **Pedron M**, **Davies KL**, **Ferreira PMDA**, **Maldonado S**, **Singer RB. 2012.** Floral features, pollination biology and breeding system of *Chloraea membranacea* Lindl. (Orchidaceae: Chloraeinae). *Annals of Botany* **110:** 1607–1621.

Schneider EL. 1979. Pollination biology of the Nymphaeaceae. *Maryland Agricultural Experiment Station Miscellaneous Publication* **1:** 419–429.

Schneider EL. 1982a. Notes on the floral biology of *Nymphaea elegans* (Nymphaeaceae) in Texas. *Aquatic Botany* **12:** 197–200.

Schneider EL. 1982b. Observations on the pollination biology of *Nymphaea gigantea* WJ Hooker (Nymphaeaceae). *The Western Australian Naturalist* **15:** 71–72.

Schneider EL. 1983. Gross morphology and floral biology on *Ondinea purpurea* den Hartog. *Australian Journal of Botany* **31:** 371–382.

Schneider EL, **Chaney T. 1981.** The floral biology of *Nymphaea odorata* (Nymphaeaceae). *The Southwestern Naturalist* **26:** 159–165.

Schneider EL, **Jeter JM. 1982.** Morphological studies of the Nymphaeaceae. XII. The floral biology of *Cabomba caroliniana*. *American Journal of Botany* **69:** 1410–1419.

Schneider EL, **Williamson PS. 1993.** Nymphaeaceae. In: Kubitzki K, Rohwer JG, Bittrich V, eds. *Flowering plants - dicotyledons. The families and genera of vascular plants.* Berlin, Heidelberg: Springer-Verlag, 486–493.

Seymour RS, **Matthews PG. 2006.** The role of thermogenesis in the pollination biology of the Amazon waterlily *Victoria amazonica*. *Annals of Botany* **98:** 1129–1135.

Stern WL, **Curry KJ**, **Pridgeon AM. 1987.** Osmophores of *Stanhopea* (Orchidaceae). *American Journal of Botany* **74:** 1323–1331.

Stpiczyńska M. 1993. Anatomy and ultrastructure of osmophores of *Cymbidium tracyanum* Rolfe (Orchidaceae). *Acta Societatis Botanicorum Poloniae* **62:** 5–9.

Stpiczyńska M. 2001. Osmophores of the fragrant orchid *Gymnadenia conopsea* L. (Orchidaceae). *Acta Societatis Botanicorum Poloniae* **70:** 91–96.

Stpiczyńska M, **Davies KL. 2016.** Evidence for the dual role of floral secretory cells in *Bulbophyllum*. *Acta Biologica Cracoviensia Series Botanica* **58:** 57–69.

Teixeira SDP, **Borba EL**, **Semir J. 2004.** Lip anatomy and its implications for the pollination mechanisms of *Bulbophyllum* species (Orchidaceae). *Annals of Botany* **93:** 499–505.

Thien LB, **Bernhardt P**, **Devall MS**, **Chen ZD**, **Luo YB**, **Fan JH**, **Yuan LC**, **Williams JH. 2009.** Pollination biology of basal angiosperms (ANITA grade). *American Journal of Botany* **96:** 166–182.

Tölke ED, **Capelli NDV**, **Pastori T**, **Alencar AC**, **Cole TC**, **Demarco D. 2019.** Diversity of floral glands and their secretions in pollinator attraction. In: Merillon JM, Ramawat K, eds. *Co-evolution of secondary metabolites. Reference series in phytochemistry*. Bordeaux: Springer, 1–46.

Valla JJ, **Cirino DR. 1972.** Biología floral del irupé, *Victoria cruziana* D'Orb. (Nymphaeaceae). *Darwiniana* **17:** 477–500.

Vogel S. 1963. Das sexuelle Anlockungsprinzip der Catasetinen- und Stanhopeen-Blüten und die wahre Funktion ihres sogenannten Futtergewebes. *Osterreichische Botanische Zeitschrift* **100:** 308–337.

Vogel S. 1990. *The role of scent glands in pollination*. Washington: Smithsonian Institution Libraries.

Vogel S, **Hadacek F. 2004.** Contributions to the functional anatomy and biology of *Nelumbo nucifera* (Nelumbonaceae) III. An ecological reappraisal of floral organs. *Plant Systematics and Evolution* **249:** 173–189.

Weryszko-Chmielewska E, **Stpiczyńska M. 1995.** Osmophores of *Amorphophallus rivieri* Durieu (Araceae). *Acta Societatis Botanicorum Poloniae* **64:** 121–129.

Wiersema JH. 1987. A monograph of *Nymphaea* subgenus *Hydrocallis* (Nymphaeaceae). *Systematic Botany Monographs* **16:** 1–112.

Wiersema JH. 1988. Reproductive biology of *Nymphaea* (Nymphaeaceae). *Annals of the Missouri Botanical Garden* **75:** 795–804.

Williamson PS, **Schneider EL. 1994.** Floral aspects of *Barclaya* (Nymphaeaceae): pollination, ontogeny and structure. *Plant Systematics and Evolution* **8:** 159–173.

Wiśniewska N, **Kowalkowska AK**, **Kozieradzka-Kiszkurno M**, **Krawczyńska AT**, **Bohdanowicz J. 2018.** Floral features of two species of *Bulbophyllum* section *Lepidorhiza* Schltr.: *B. levanae* Ames and *B. nymphopolitanum* Kraenzl. (Bulbophyllinae Schltr., Orchidaceae). *Protoplasma* **255:** 485–499.

Zarlavsky GE. 2014. *Histología vegetal. Técnicas simples y complejas.* Buenos Aires: Boletín de la Sociedad Argentina de Botánica.

Zini LM, **Galati BG**, **Ferrucci MS. 2017.** Perianth organs in Nymphaeaceae: comparative study on epidermal and structural characters. *Journal of Plant Research* **130:** 1047–1060.